

Isospin dependence of isobaric ratio $Y(^3\text{H})/Y(^3\text{He})$ and its relation to temperature

M. Veselsky^{1,2}, R. W. Ibbotson³, R. Laforest⁴,
E. Ramakrishnan⁵, D. J. Rowland⁴, A. Ruangma,
E. M. Winchester, E. Martin and S. J. Yennello

*Cyclotron Institute, Texas A&M University, College Station, TX 77843-3366,
USA*

Abstract

A dependence of the isobaric ratio $Y(^3\text{H})/Y(^3\text{He})$ on the N/Z ratio of the reconstructed quasiprojectile for the reaction of ^{28}Si beam with $^{112,124}\text{Sn}$ targets at two different projectile energies of 30 and 50 MeV/nucleon is presented. We demonstrate a linear dependence of the observable $\ln(Y(^3\text{H})/Y(^3\text{He}))$ on the N/Z ratio of the quasiprojectile and show the dependence of the slope on the reconstructed excitation energy of the quasiprojectile. We relate this slope dependence at a given excitation energy to the temperature of the fragmenting system. Using the model assumptions of the statistical multifragmentation model, a method of temperature determination is proposed. A caloric curve is constructed and compared to the result of the double isotope ratio method for the same set of the data and to the results of other studies.

Key words: Projectile multifragmentation; Isospin dependence; Caloric curve
PACS: 25.70.Mn, 25.70.Pq, 25.70.-z

Multifragmentation of highly excited nuclei has been subject of significant interest for many years. Since the nuclei are two-component systems consisting of protons and neutrons, the influence of isospin on the disassembly of hot nuclei is a question of general interest. Experimental studies have demonstrated the influence of the isospin of projectile and target on the isotopic

¹ Phone: (979)-845-1411, fax: (979)-845-1899, e-mail: veselsky@comp.tamu.edu

² On leave of absence from Institute of Physics of SASc, Bratislava, Slovakia

³ Present address: Brookhaven National Laboratory, Brookhaven, New York, USA

⁴ Present address: Mallinckrodt Institute of Radiology, St. Louis, Missouri, USA

⁵ Present address: Microcal Software Inc, One Roundhouse Plaza, Northampton, MA 01060, USA

yields of fragments [1–5]. Theoretical framework for fragmentation of asymmetric systems have been developed [6–11] and a possible phase transition into an isospin-symmetric liquid and an isospin-asymmetric gas phase have been suggested. In our recent work [12] we presented the characteristics of the quasiprojectiles with $Z = 12 - 15$, reconstructed from the fully isotopically resolved fragments with $Z_f \leq 5$, detected in the forward angles using the FAUST multidetector array [13] at Cyclotron Institute of Texas A&M University. The distributions of the quasiprojectile velocity, mass, charge and excitation energy were obtained in the reaction of a ^{28}Si beam with $^{112,124}\text{Sn}$ targets at projectile energies 30 and 50 MeV/nucleon. We demonstrated that these experimental observables of the quasiprojectile can be reproduced satisfactorily by hybrid simulations, using a code implementing the model of deep inelastic transfer [14] for a calculation of the properties of excited quasiprojectiles and the SMM code [15] for a description of multifragmentation of excited quasiprojectiles. Further details can be found in [12]. The level of an agreement obtained implies that the influence of the non-statistical effects caused by violent collisions of the projectile and the target on the properties of detected quasiprojectiles can be practically excluded for the selected events. The obtained set of data allows further study of thermal quasiprojectile multifragmentation, especially the study of the influence of the quasiprojectile isospin on the properties of fragmenting system. This data is of specific interest because the isospin of the system which actually undergoes multifragmentation is known with good precision. The first part of the study was presented in our recent work [16] where multiplicities and N/Z ratios of light charged particles (LCPs) and intermediate mass fragments (IMFs) were studied. Different trends of multiplicities and an inhomogeneous distribution of isospin between light charged particles and intermediate mass fragments were observed. The multiplicity of LCPs increases rapidly with proton excess, while the multiplicity of IMFs increases slowly with increasing neutron number. For quasiprojectiles with large proton excess an inhomogeneous distribution of isospin into proton-rich LCPs and more symmetric IMFs occurs. Furthermore, dependences of the isobaric ratio $Y(^3\text{H})/Y(^3\text{He})$ on the N/Z ratio (as a variable closely connected to isospin) and on the excitation energy of the reconstructed quasiprojectiles were presented in [16]. In this work we will present a detailed study of the trends of the isobaric ratio $Y(^3\text{H})/Y(^3\text{He})$. The relationship of $Y(^3\text{H})/Y(^3\text{He})$ to thermodynamical observables will be discussed.

The dependences of the isobaric ratio $Y(^3\text{H})/Y(^3\text{He})$ on the N/Z ratio of the quasiprojectile (N/Z_{QP}) are shown in Fig. 1 for the reaction of a ^{28}Si beam with $^{112,124}\text{Sn}$ targets at projectile energies of 30 and 50 MeV/nucleon. The quasiprojectiles with $Z = 12 - 15$, reconstructed from the fully isotopically resolved charged fragments with $Z_f \leq 5$, are selected (for details of the experiment see [12,17]). Various symbols represent the experimental data for different targets at each beam energy. The data within each set form nearly straight lines thus implying an exponential dependence of the isobaric ratio

$Y(^3\text{H})/Y(^3\text{He})$ on N/Z_{QP} . For a given projectile energy, the $Y(^3\text{H})/Y(^3\text{He})$ dependence on N/Z_{QP} is practically identical for the two different targets $^{112,124}\text{Sn}$. This shows that the isotopic trends are determined by the isospin of the excited system which fragments and the trends obtained by comparison of the data for different projectile-target systems describe only the overall trends. A detailed discussion of this issue is in our previous work [16]. For the two different projectile energies 30 and 50 MeV/nucleon the $Y(^3\text{H})/Y(^3\text{He})$ dependence exhibits a different slope. In the above mentioned work [12], the distributions of the apparent excitation energy (E_{app}^*) are practically identical for the different targets at a given projectile energy and shift to the increasing values of E_{app}^* with an increasing beam energy. The mean values of E_{app}^* are 101.2 and 102.3 MeV for ^{112}Sn and ^{124}Sn targets at the projectile energy 30 MeV/nucleon and 142.8 MeV for both targets at the projectile energy 50 MeV/nucleon. Such a similarity may imply that the slope of the dependence of isobaric ratio $Y(^3\text{H})/Y(^3\text{He})$ on N/Z_{QP} correlates with the mean excitation energy of the quasiprojectile. Preliminary indications of this dependence have been reported in ref. [16]. This assumption may be examined by extracting the isobaric ratio $Y(^3\text{H})/Y(^3\text{He})$ for different bins of the apparent excitation energy of the quasiprojectile.

Fig. 2 shows the dependences of the isobaric ratio $Y(^3\text{H})/Y(^3\text{He})$ on N/Z_{QP} for the nine bins of the apparent excitation energy per mass unit of the quasiprojectile (ϵ_{app}). The data for both targets and projectile energies were combined to increase the statistics. This is possible because for a given excitation energy bin, the $Y(^3\text{H})/Y(^3\text{He})$ dependences agree within the statistical deviations. The squares represent the experimental data and the lines are the fits obtained using the MINUIT minimization package [18]. As one can see on Fig. 2, linearity is the overall feature of the logarithmic plots of the $Y(^3\text{H})/Y(^3\text{He})$ ratio in all excitation energy bins and is especially significant in the excitation energy bins with a high statistics. The slopes are steepest at low excitation energies and become flatter with increasing excitation energy.

Since the experimental dependences of the isobaric ratio $Y(^3\text{H})/Y(^3\text{He})$ on N/Z_{QP} correlate with ϵ_{app} and are linear on a logarithmic scale (and thus depend exponentially on N/Z_{QP}), it would be of interest to relate the slope to the thermodynamical observables of the quasiprojectile multifragmentation. As a starting point we chose the statistical multifragmentation model (SMM) [15] which was employed in the simulation successfully describing our data [12,16]. In the macrocanonical approach, the SMM gives the mean number of the emitted fragments of a given N_k and Z_k as

$$\langle M_{N_k Z_k} \rangle = g_{N_k Z_k} \frac{V_f}{\lambda_T^3} A^{3/2} \exp\left(\frac{F_{N_k Z_k}(T, V) - \mu_n N_k - \mu_p Z_k}{T}\right) \quad (1)$$

where T is the freeze-out temperature, V is the freeze-out volume, $g_{N_k Z_k}$ is

the degeneracy of the fragment ground state, V_f is the free volume available for translational motion of the fragment, λ_T is the thermal wavelength of the nucleon, $F_{N_k Z_k}(T, V)$ is the internal free energy of the fragment and μ_n and μ_p are the chemical potentials for neutrons and protons. The assumption of chemical equilibrium is not incorporated into SMM [15] and the chemical potentials μ_n and μ_p are used as a Lagrange multipliers ensuring the conservation of the mean neutron and proton number. When considering the isospin dependence of the experimental $Y(^3\text{H})/Y(^3\text{He})$ ratio for a given excitation energy bin, the exponential dependence suggests a possibility to determine a single temperature for each bin as a simplest possible interpretation. The isobaric ratio $Y(^3\text{H})/Y(^3\text{He})$ then can be determined as

$$\frac{Y(^3\text{H})}{Y(^3\text{He})} = \frac{\langle M_{21} \rangle}{\langle M_{12} \rangle} = \exp\left(-\frac{F_{21}(T, V) - F_{12}(T, V) - \mu_n + \mu_p}{T}\right) \quad (2)$$

where we used the fact that V_f and λ_T are the same for the whole partition and that the ground state spins of both fragments are equal.

We approximate the $\mu_n - \mu_p$ by the difference in the neutron (S_n) and proton (S_p) ground state separation energy. According to the model of a nuclear Fermi gas at zero temperature, S_n and S_p can be identified with the chemical potentials for protons and neutrons in the ground state. When introducing finite temperature, the Fermi gas model predicts only a moderate change of the chemical potential for temperatures well below the Fermi energy. Thus the approximation of chemical potentials by separation energies can be still considered valid for highly excited thermally equilibrated nuclei and determines the correct chemical potentials prior to multifragmentation. During multifragmentation the system expands which creates two different trends. When considering the system as Fermi gas expanding to the freeze-out density (typically $0.4\rho_0$ for the present case according to the formula used in the SMM), the values of the Fermi energy decrease by more than 40 %. The same behavior can be expected also for $\mu_n - \mu_p$. On the other hand, chemical potentials of nucleons are influenced by the process of multifragmentation. As reported in our previous work [16], the IMFs are more isospin-symmetric than light charged particles. Within statistical multifragmentation model, the isobaric ratio $Y(^3\text{H})/Y(^3\text{He})$ can be identified with the ratio of mean densities of free neutrons and protons for a given fragment partition (as one can see after dividing equation 1 by freeze-out volume). As follows from Figs. 1,2, such ratios differ dramatically from the starting values and one can expect also the values of $\mu_n - \mu_p$ significantly higher than those of an expanded Fermi gas. When assuming that both effects have similar magnitude, the approximation used can be considered as a reasonable estimate of the actual values. For the full set of data used in Fig.2, $\mu_n - \mu_p$ can be approximated as

$$\mu_n - \mu_p \approx S_p - S_n = (-43.44 \pm 0.97) + (38.57 \pm 0.94)N/Z_{QP} \text{ [MeV]}. \quad (3)$$

Experimental mass excesses [19] have been used for the evaluation. The dependence of $S_n - S_p$ on the N/Z ratio of the quasiprojectile can be considered linear with good precision. The difference in the internal free energy of the fragments ${}^3\text{H}$ and ${}^3\text{He}$, according to the evaluation formulas given in [15], is of the order of a few hundred keV on a broad range of N/Z_{QP} and changes much more slowly than $\mu_n - \mu_p$. In this paper we neglect its weak dependence on N/Z_{QP} and treat it as a constant independent on N/Z_{QP} . Within our approximation, the resulting expression for the isobaric ratio $Y({}^3\text{H})/Y({}^3\text{He})$ will be

$$\ln(Y({}^3\text{H})/Y({}^3\text{He})) = \ln(K(T)) + (\mu_n - \mu_p)/T \quad (4)$$

where $K(T)$ is a proportionality factor dependent on the temperature but independent of the N/Z ratio of the fragmenting system. According to the evaluation formulas for the free energy given in [15], one may expect the values of proportionality factor $K(T)$ to be close to unity.

Since both $\ln(Y({}^3\text{H})/Y({}^3\text{He}))$ and $\mu_n - \mu_p$ depend linearly on N/Z_{QP} (as may be seen from Fig. 2 and equation 3) and since we choose the value of $\ln(K(T))$ to be a constant, independent of N/Z_{QP} , the expressions on both sides of equation 4 are in fact first order polynomials of N/Z_{QP} . Then the solution is obvious, constants and coefficients of first order (slopes) should be equal on both sides of the equation. This allows a determination not only of the temperature (as a ratio of the slopes) but also of $\ln(K(T))$ from the comparison of the zero order coefficients (constants) using the extracted temperature. The resulting values of T and $\ln(K(T))$ are given in Fig. 3 and Fig. 4 for the different quasiprojectile excitation energy bins. The numerical values of T and $\ln(K(T))$ are given in the Table 1 along with the parameters of the linear fits of $\ln(Y({}^3\text{H})/Y({}^3\text{He}))$ given in Fig. 2. The dependence of the temperature on the excitation energy (caloric curve) given in Fig. 3 (solid squares) is compared to the experimental caloric curve obtained for the same set of the data by the double isotope ratio method [20,21] for the thermometer $d,t/{}^3\text{He},{}^4\text{He}$ (the dashed line indicates the double isotope ratio temperature and the solid lines indicate the statistical errors). The formula

$$T_{d,t/{}^3\text{He},{}^4\text{He}} = 14.31\text{MeV} / \ln(1.59 \frac{Y({}^2\text{H})/Y({}^3\text{H})}{Y({}^3\text{He})/Y({}^4\text{He})}) \quad (5)$$

was used for the calculations. The agreement between the two plots is reasonable. Both methods give the value of the temperature between 5 and 7 MeV for the apparent excitation energies above 5 MeV/nucleon. Similar values of the temperature are reported by other experimental studies [22–25]. The values of the temperature predicted by the SMM [15] are also in the same range. The values of $\ln(K(T))$ are between 0 and 1 and suggest the values of $K(T)$

between 1 and 3, which are in good agreement with the values of the SMM. The dependence of $\ln(K(T))$ on the temperature is quite weak, which is also consistent with the expectations. Large relative errors of the $\ln(K(T))$ values are caused by the subtraction of numbers of similar magnitude. The agreement between temperatures determined by two different methods shows that the assumptions made for $\mu_n - \mu_p$ reflect the physical trends which take place in the freeze-out configuration.

Since the neutron emission from the quasiprojectile is not included in the data presented here, we tried to estimate its influence. Using a backtracing procedure described in [12], we estimated the initial values of the excitation energy of a hot quasiprojectile at the stage where it also includes the neutrons that are later emitted. The mean value of the excitation energy taken away by a neutron emission ranges from 0.5 MeV/nucleon for the highest bin of ϵ_{app} to 1.5 MeV/nucleon for the lowest bin. This applies to both methods of the temperature determination presented here and implies that the events represent a still broader range of the initial excitation energies of the quasiprojectile. Since the multiplicity of the charged fragments decreases with decreasing ϵ_{app} , the decrease of the determined temperatures in the lowest bins of ϵ_{app} may be a signature of the onset of a low energy deexcitation mode where several neutrons and light charged particles are emitted prior to the breakup of the partially cooled residue into two massive fragments (such a mass distribution is observed in the channels with 3 and 4 charged fragments). The temperatures determined thus become mean values representing the range of temperatures at which hydrogen and helium isotopes are emitted during the deexcitation cascade. The use of ${}^3\text{He}$ for the evaluation of the isobaric ratio $Y({}^3\text{H})/Y({}^3\text{He})$ could be affected by the so-called ${}^3\text{He}$ -puzzle (see [26]), nevertheless it appears that the ${}^3\text{He}$ -anomaly is not relevant for peripheral collisions induced by light projectile nuclei.

We presented the dependence of the isobaric ratio $Y({}^3\text{H})/Y({}^3\text{He})$ on N/Z_{QP} for the reaction of a ${}^{28}\text{Si}$ beam on ${}^{112,124}\text{Sn}$ targets at two different projectile energies 30 and 50 MeV/nucleon. We demonstrated a linear dependence of $\ln(Y({}^3\text{H})/Y({}^3\text{He}))$ on N/Z_{QP} and the dependence of the slope on the excitation energy of the quasiprojectile. Using the model assumptions of the statistical multifragmentation model, we demonstrated the possibility of relating the slope of the dependence of $\ln(Y({}^3\text{H})/Y({}^3\text{He}))$ on N/Z_{QP} to the temperature at a given excitation energy. We constructed a caloric curve and demonstrated its equivalence to the results of the double isotope ratio method. Our results show that the temperatures extracted from the isospin dependence of $Y({}^3\text{H})/Y({}^3\text{He})$ are consistent with the temperature of the freeze-out configuration where thermal equilibration occurs. The approximation used for the evaluation of the difference of neutron and proton chemical potentials is consistent with significant changes of densities of neutrons and protons during multifragmentation.

The authors wish to thank the Cyclotron Institute staff for the excellent beam quality. This work was supported in part by the NSF through grant No. PHY-9457376, the Robert A. Welch Foundation through grant No. A-1266, and the Department of Energy through grant No. DE-FG03-93ER40773. M. V. was partially supported through grant VEGA-2/5121/98.

References

- [1] R. Wada et al., *Phys. Rev. Lett.* **58** (1987) 1829.
- [2] S.J. Yennello et al., *Phys. Lett.* **B 321** (1994) 15.
- [3] H. Johnston et al., *Phys. Lett.* **B 371** (1996) 186.
- [4] H. Johnston et al., *Phys. Rev.* **C 56** (1997) 1972.
- [5] E. Ramakrishnan et al., *Phys. Rev.* **C 57** (1998) 1803.
- [6] D.Q. Lamb, J.M. Lattimer, C.J. Pethick and D.G. Ravenhall, *Nucl. Phys.* **A 360** (1981) 459.
- [7] H. Müller and B.D. Serot, *Phys. Rev.* **C 52** (1995) 2072.
- [8] Ph. Chomaz and F. Gulminelli, *Phys. Lett.* **B 447** (1999) 221.
- [9] B.A. Li and C.M. Ko, *Nucl. Phys.* **A 618** (1997) 498.
- [10] V. Baran, M. Colonna, M. Di Toro and A.B. Larionov, *Nucl. Phys.* **A 632** (1998) 287.
- [11] H.W. Barz et al., *Phys. Lett.* **B 211** (1988) 10.
- [12] M. Veselsky et al., *Phys. Rev.* **C 62** (2000) 64613.
- [13] F. Gimeno-Nogues et al., *Nucl. Inst. and Meth. In Phys. Res.* **A 399** (1997) 94.
- [14] L. Tassan-Got and C. Stéfan, *Nucl. Phys.* **A 524** (1991) 121.
- [15] J.P. Bondorf, A.S. Botvina, A.S. Iljinov, I.N. Mishustin and K. Sneppen, *Phys. Rep.* **257** (1995) 133.
- [16] M. Veselsky et al., *Phys. Rev.* **C 62** (2000) 41605.
- [17] R. Laforest et al., *Phys. Rev.* **C 59** (1999) 2567.
- [18] F. James and M. Roos, MINUIT – Users Guide, Program Library D506, CERN, 1981.
- [19] G. Audi and A.H. Wapstra, *Nucl. Phys.* **A 595** (1995) 409.
- [20] S. Albergo et al., *Nuovo Cimento* **89** (1995) 1.

- [21] A. Kolomiets, V.M. Kolomietz and S. Shlomo, *Phys. Rev. C* **55** (1997) 1376.
- [22] J. Pochodzalla et al., *Phys. Rev. Lett.* **75** (1995) 1040.
- [23] J.A. Hauger et al., *Phys. Rev. Lett.* **77** (1995) 235.
- [24] A. Schuttauf et al., *Nucl. Phys. A* **607** (1996) 457.
- [25] H. Xi et al., *Z. Phys. A* **359** (1997) 397.
- [26] W. Neubert and A.S. Botvina, *Eur. Phys. J. A* **7** (2000) 101.

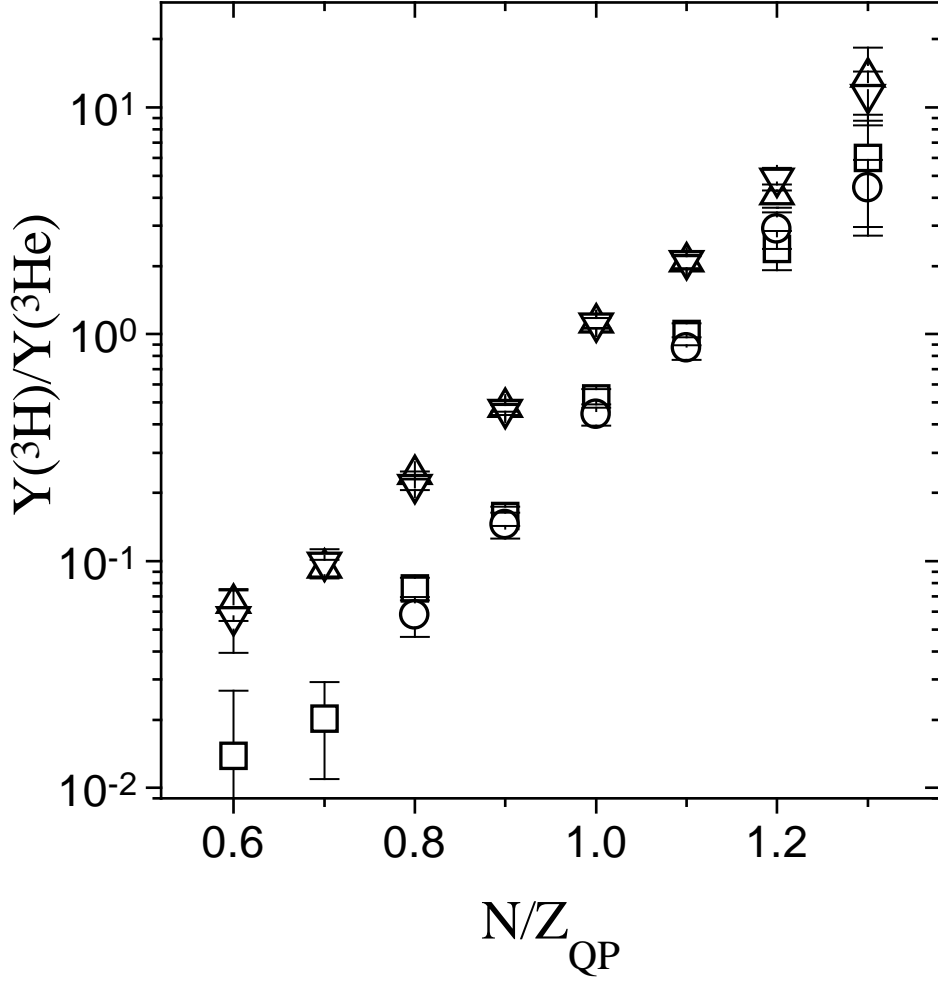


Fig. 1. Dependence of the isobaric ratio $Y(^3\text{H})/Y(^3\text{He})$ on the N/Z ratio of the fully isotopically resolved quasiprojectiles with $Z_{tot} = 12 - 15$. Squares - $^{28}\text{Si}(30\text{MeV/nucleon})+^{112}\text{Sn}$, circles - $^{28}\text{Si}(30\text{MeV/nucleon})+^{124}\text{Sn}$, up triangles - $^{28}\text{Si}(50\text{MeV/nucleon})+^{112}\text{Sn}$, down triangles - $^{28}\text{Si}(50\text{MeV/nucleon})+^{124}\text{Sn}$.

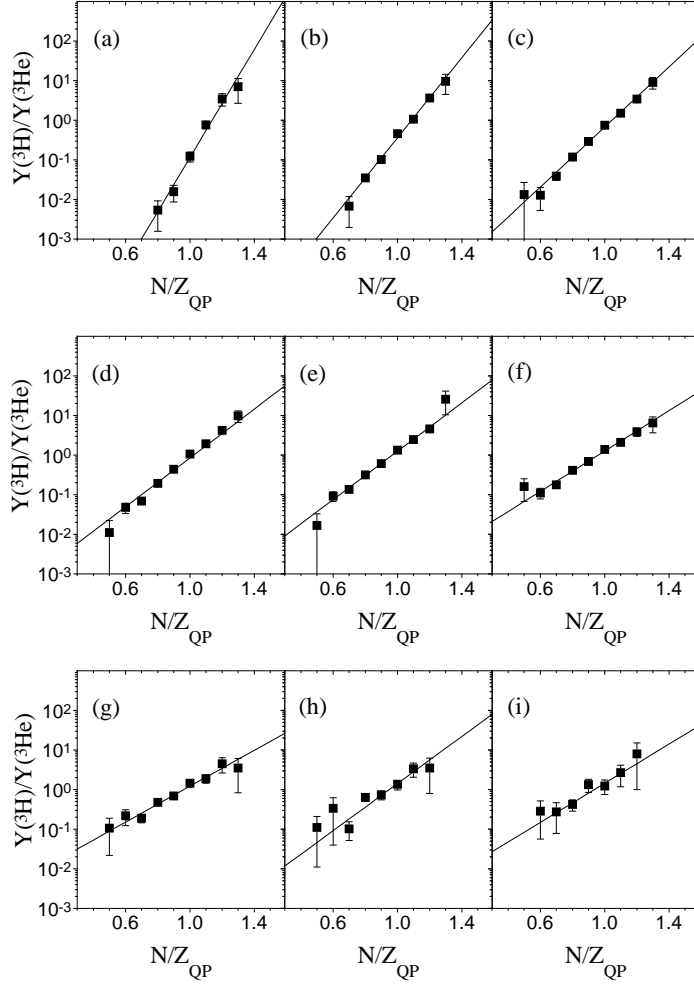


Fig. 2. Dependence of the isobaric ratio $Y(^3\text{H})/Y(^3\text{He})$ on the N/Z ratio of the fully isotopically resolved quasiprojectiles with $Z_{tot} = 12 - 15$ for the different bins of ϵ_{app} . The panels (a) - (i) correspond to the excitation energy bins given in Table 1. The full set of the data from reactions of ^{28}Si beam with $^{112,124}\text{Sn}$ targets at the projectile energies 30 and 50 MeV/nucleon was used.

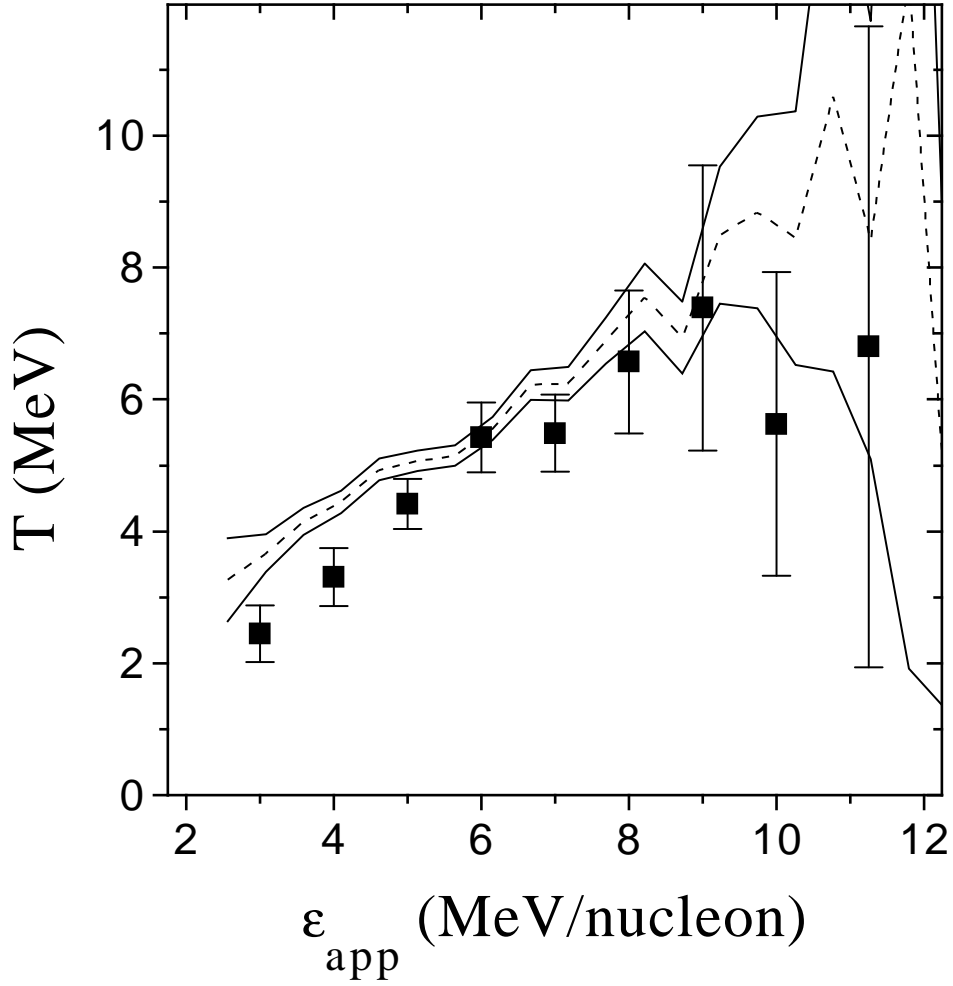


Fig. 3. Dependence of the temperature T , determined from the dependence of the isobaric ratio $Y(^3\text{H})/Y(^3\text{He})$ on the N/Z ratio of the fragmenting quasiprojectile, on ϵ_{app} (solid squares). Dashed and solid lines indicate the values and the statistical deviations of the temperature determined using the double isotope ratio method for the thermometer $d,t/^3\text{He},^4\text{He}$.

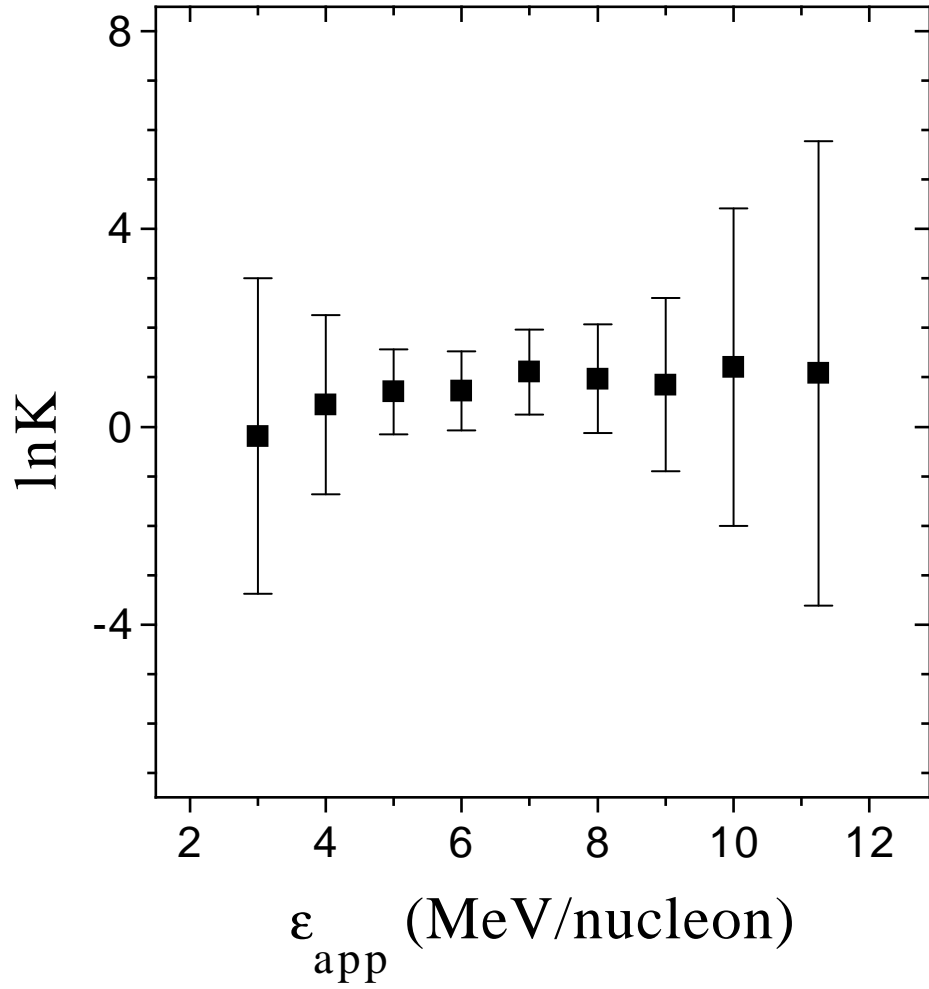


Fig. 4. Dependence of $\ln(K(T))$, determined from the dependence of the isobaric ratio $Y(^3\text{H})/Y(^3\text{He})$ on N/Z_{QP} , on ϵ_{app} .

Table 1

Parameters of the exponential fit $\frac{Y(^3\text{H})}{Y(^3\text{He})} = \exp(a_1 + a_2(\frac{N}{Z})_{QP})$ for the different bins of the apparent excitation energy ϵ_{app} and the determined values of the temperature T and $\ln(K(T))$ for the same bins.

ϵ_{app} , MeV/nucleon	a_1	a_2	T , MeV	$\ln(K(T))$
2.5-3.5	-17.895±2.170	15.719±2.007	2.45±0.43	-0.19±3.19
3.5-4.5	-12.665±1.175	11.642±1.160	3.31±0.44	0.45±1.81
4.5-5.5	-9.124±0.517	8.730±0.538	4.42±0.38	0.71±0.86
5.5-6.5	-7.267±0.483	7.099±0.515	5.43±0.53	0.73±0.80
6.5-7.5	-6.808±0.518	7.031±0.564	5.49±0.58	1.11±0.86
7.5-8.5	-5.634±0.682	5.868±0.744	6.57±1.08	0.97±1.10
8.5-9.5	-5.023±1.084	5.218±1.210	7.39±2.16	0.85±1.75
9.5-10.5	-6.499±2.020	6.846±2.202	5.63±2.30	1.21±3.21
10.5-12.5	-5.323±2.931	5.689±3.241	6.80±4.86	1.08±4.69